

Collision-induced rovibrational spectra of H₂-He pairs from first principles

Lothar Frommhold

Physics Department, University of Texas at Austin, Austin, Texas 78712-1081

Wilfried Meyer

Fachbereich Chemie der Universität, D-675 Kaiserslautern, West Germany

(Received 22 August 1986)

A previous study of the collision-induced dipole moment has treated the H₂-He complex as a molecule in self-consistent-field and size-consistent coupled-electron-pair approximation [Meyer and Frommhold, *Phys. Rev. A* **34**, 2771 (1986)]. Based on that work, the vibrational dipole transition elements $\langle v | A_{\lambda L}(R, r) | v' \rangle$ associated with the fundamental band ($v=0 \rightarrow v'=1$) are obtained as functions of separation R of the collisional pair for the isotropic and anisotropic overlap induction components ($\lambda L=01$ and 21), and the quadrupole- and hexadecapole-induced parts ($\lambda L=23$ and 45). From these induced dipole components and Meyer, Hariharan, and Kutzelnigg's isotropic part of the *ab initio* potential surface, we compute in the (forbidden) fundamental band of hydrogen the collision-induced absorption spectra of the collisional complex of hydrogen (H₂) and helium from an exact quantum formalism. Both the shape of the computed spectral profiles and the theoretical absolute intensity agree closely with existing measurements at temperatures from 18 to 300 K. The fact that these spectra, and presumably the analogous overtone and "hot" ($v > 0$) bands of the H₂-He complex which are not known from measurements, can be accurately obtained from basic principles is significant for research related to the atmospheres of the giant planets and late-type stars.

INTRODUCTION

In an attempt to record an infrared vibration spectrum of the (O₂)₂ van der Waals dimer, Welsh and his associates discovered a new type of spectra, namely, those of collisional complexes of molecules.^{1,2} Such supermolecular spectra are commonly observed in absorption and are referred to as collision-induced absorption (CIA) spectra. Even if only nonpolar collisional partners are involved, intermolecular interactions usually induce transient dipole moments which in turn generate such spectra. The short "lifetime" ($\sim 10^{-12}$ sec) of a collisional pair is responsible for the observed great width ($\sim 10^{12}$ Hz) of CIA spectra.

Several mechanisms are known by which a dipole moment is induced during collisional interactions. Usually the most important one is the polarization of the collisional partner in the electric multipole field of a molecule, but other induction mechanisms related to exchange and dispersion forces are also effective if dissimilar collisional partners are involved. Since induced dipole moments are dependent on the vibrational and rotational coordinates of the molecules, besides being functions of the separation of the collisional pair, CIA spectra occur at certain (forbidden) rovibrational frequencies of the molecules involved. Accordingly, we distinguish rototranslational and rovibrational CIA spectra. The latter variety is further subdivided into fundamental, overtone, and "hot" ($v > 0$) bands.

CIA spectra of nonpolar gases and gas mixtures have been investigated over a great range of densities and temperatures, and in all frequency regions. It is clear that near the low-density limit (and at not too low frequencies³) the spectra of the *binary* collisional complexes dominate the observation but at high densities (~ 100 amagat

or more), the effects of many-body interactions cannot be ignored.²

CIA spectra are of interest for the information on intermolecular interactions obtainable from them. Furthermore, collision-induced dipoles have been shown to provide significant sources of opacity in planetary atmospheres^{4,5} and late-type stars.⁶ It has been argued that the differences between the H₂-He and H₂-H₂ CIA spectra should provide an intriguing device for the measurement of the [He]/[H₂] abundance ratio.⁷ For all of these reasons, a treatment of such spectra based on first principles is of interest, especially where theoretical results can be compared with dependable measurements. From the standpoint of the quantum chemist, the simplest system to consider which is also of some practical importance is the He-Ar pair. It has been recently treated as a molecule in self-consistent-field (SCF) and size-consistent coupled-electron-pair approximation (CEPA) computations⁸ which avoid the basis-set superposition errors encountered in previous work. From the *ab initio* induced dipole moment, translational CIA spectra have been computed using an exact quantum formalism.^{9,10} Both the shape and the intensity of these theoretical spectra are in close agreement with existing measurements; no adjustable parameters of any sort have been employed in that comparison.⁹ We note that the uncertainty of the computed dipole moments and CIA spectra is probably less than $\sim 5\%$ so that theory rivals the precision attainable with the best spectroscopic measurements.

In a subsequent study, the H₂-He collisional pair has been treated similarly.¹¹ The basis set adopted accounts for 95% of the correlation energy. As a first step, the vibrational average of the induced dipole moment of the hydrogen ground state ($v=v'=0$) was obtained and em-

ployed for a calculation of the rototranslational CIA spectra.¹¹ These were found to be in close agreement with existing measurements of these spectra at temperatures from 77 to ~300 K. In the present work, we will consider the CIA spectra involving vibrational transitions from the hydrogen ground state ($v=0$) to the lowest excited vibrational state ($v'=1$) of H₂. The enhancement by helium of the collision-induced fundamental band of hydrogen is well known from several measurements to be reviewed below.^{2,12} Corresponding overtone and hot bands can in principle also be obtained from the published work¹¹ but, since for the H₂-He pair no measurements of such spectra exist, we will limit the present study to the fundamental band.

We consider here the binary or "intracollisional" spectra. This means that, in particular, we will ignore the various observed "dips" due to *intercollisional* interference¹³ which have been discussed elsewhere.¹⁴⁻¹⁷ Intercollisional interference is a many-body effect which does not exist in a binary system.

INDUCED DIPOLE MOMENT

The details of the SCF and CEPA computations of the induced dipole moment μ as function of the molecular orientation (δ), the H₂-He separation (\mathbf{R}), and the vibrational spacing of the H₂ molecule (\mathbf{r}) have been communicated elsewhere.¹¹ The results are listed in Table III of Ref. 11. These need to be recast in terms of the expansion coefficients $A_{\lambda L}(r, R)$ defined by

$$\mu_\nu(\mathbf{r}, \mathbf{R}) = \frac{4\pi}{\sqrt{3}} \sum_{L, \lambda} A_{\lambda L}(r, R) \sum_m Y_\lambda^m(\hat{\mathbf{r}}) Y_L^{v-m}(\hat{\mathbf{R}}) \times C(\lambda L 1; m, v-m). \quad (1)$$

In this expression, $\hat{\mathbf{r}}$ and $\hat{\mathbf{R}}$ are unit vectors in the directions of molecular orientation and intermolecular separation. We note that for molecules with inversion symmetry the expansion parameter λ is an even non-negative integer. The Y are spherical harmonics. The subscript $L=1, 3, \dots$ is odd because of the transformation properties of dipole components. Furthermore, we have $L=\lambda \pm 1$ from the triangular inequalities. From the induced dipole components μ_ν ($\nu=0, \pm 1$), which were computed at three different orientations, 0°, 45°, and 90°, the four expansion coefficients $A_{\lambda L}$ with $\lambda L=01, 21, 23$, and 45 can thus be obtained as functions of r and R ; higher terms are negligible. From the results we compute the vibrational matrix elements

$$B_{\lambda L}^{v v'}(R) = \langle v | A_{\lambda L}(r, R) | v' \rangle \quad (2)$$

using vibrational wave functions of H₂ based on Kolos and Wolniewicz's *ab initio* potential.¹⁸ The $B_{\lambda L}^{01}(R)$ may be considered spherical tensor components of the dipole moment for transitions from the vibrational ground state ($v=0$) to the lowest excited state ($v'=1$). (Previous work¹¹ has considered the vibrational average of the ground state, $v=v'=0$.) Henceforth, we will drop the superscripts v, v' for convenience.

Figure 1 shows how the pure overlap components B_{01} and B_{21} fall off roughly exponentially with separation.

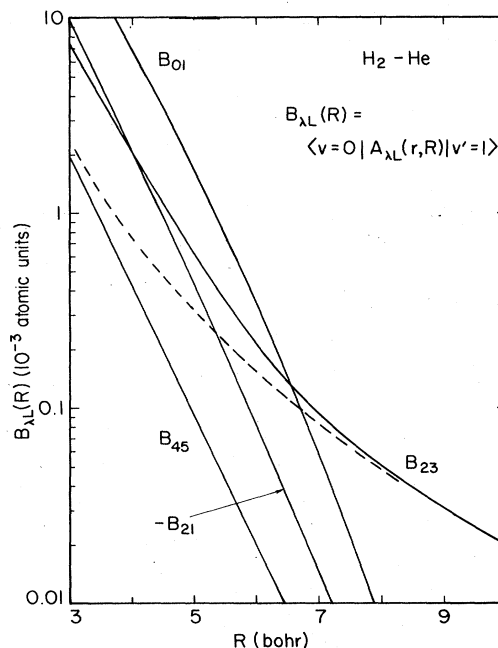


FIG. 1. Vibrational matrix elements of the induction coefficients $A_{\lambda L}(r, R)$, as needed for the computation of the fundamental band, $v=0 \rightarrow v'=1$, of the H₂-He collisional pair. The dashed curve represents the pure quadrupole induction, Eq. (3), for comparison.

At long range ($R > 7$ bohrs), the quadrupole-induced B_{23} component dominates and approximates quite closely the pure quadrupole induction,

$$B_{23}(R) \simeq \sqrt{3} \alpha(\text{He}) q_2(\text{H}_2) / R^4 \quad (\text{for } R \rightarrow \infty). \quad (3)$$

Here, $\alpha(\text{He})=1.385$ a.u. is the polarizability of helium¹⁹ and

$$q_2(\text{H}_2) = \langle v=0 | q_2(r) | v'=1 \rangle = 0.2085 \text{ a.u.}$$

is the quadrupole matrix element²⁰ associated with vibrational transitions $v=0 \rightarrow v'=1$. However, at near range, the B_{23} component differs substantially from the extrapolation to small R of the asymptotic expression (dashed curve, Fig. 1). The hexadecapole-induced term $B_{45}(R)$ is so weak that its contributions to the observable spectra may not be discernible in an actual measurement.

Table I lists the $B_{\lambda L}$ components for $v=0 \rightarrow v'=1$ as

R	$\lambda L=01$	23	21	45
3	25 283	7644	-10 178	2021
4	7043	2129	-2210	450
5	1731	632	-450	93
6	356	219	-82	20
7	58	96	-15	6
8	4	51	-3	2
10	-2	20	0	0

TABLE II. Coefficients in Eq. (4), with $R_0=5.80$ bohrs.

λL	N	C_N	c_2	c_3	c_4
01	7	-18.4	0.000 569	-1.5801	-0.046 25
21		0	-0.000 118	-1.6870	-0.032 87
23	4	0.2019	0.000 088 5	-1.5994	-0.051 77
45	6	0.482	0.000 014 7	-1.9051	-0.101 61

function of separation. It is convenient to represent these values by an analytical expression of the form

$$B_{\lambda L}(R) = \frac{C_n}{R^n} + c_2 \exp[c_3(R - R_0) + c_4(R - R_0)^2], \quad (4)$$

with $R_0=5.80$ bohrs (which is roughly equal to the collision diameter, $\sigma=5.75$ bohrs). The coefficients c_1 , C_n are given in Table II. It is difficult to assess a dependable uncertainty limit for the computed coefficients $B_{\lambda L}$, but the errors are probably less than a few percent; see a discussion in Ref. 11 and the comparison with measurements below.

Wormer and van Dijk have previously obtained values of the $B_{\lambda L}(R)$ for $v=0 \rightarrow v'=1$, using SCF-type calculations.²¹ They find a B_{01} coefficient which at the separation of $R=3$ bohrs is in agreement with our results. With increasing separation R , however, not surprisingly, their B_{01} value is increasingly greater than our results which include the (negative) dispersion interaction not accounted for in the previous work. We note that even if we subtract the leading dispersion term C_7/R^7 from our $B_{01}(R)$ values, Wormer and van Dijk's B_{01} coefficient is $\sim 25\%$ stronger at $R=6$ bohrs. The overlap part of B_{23} is also in agreement with our work at $R=4.5$ bohrs but falls off more slowly with separation. The B_{21} component is, contrary to our results, not well approximated by an exponential function and thus in lesser agreement with our work.

Since for the B_{01} and B_{21} terms the C_n coefficients are quite small, we have a nearly exponential falloff of the overlap components, with a logarithmic slope of roughly $\rho = -1/c_3 \approx 0.63$ bohrs. Empirical work²² has indicated a consistent value of $\rho=0.624$ bohrs. Besides empirical range parameters, a few empirical overlap strength parameters have been quoted. From an analysis of the $Q_1(1)$ branch, Poll and Hunt²² quote $B_{01}=0.00094$ a.u. at $R=5.18$ bohrs, to be compared with our value of 0.0013 a.u. at the same separation. In the derivation of the dipole strength, a choice of the interaction potential, a Lennard-Jones 6-12 model with $\sigma=5.18$ bohrs (instead of the accurate $\sigma=5.75$ bohrs) was made which is now known to be a poor description of the H_2 -He interaction. Computed spectral moments turn out much greater when smaller σ values are employed, which explains the difference between the empirical and the *ab initio* values. From a study of the $S_1(1)$ line and with the assumption $\rho=0.52$ bohrs (which is too small according to our results), Poll *et al.*²³ obtain $B_{21}=0.25 \times 10^{-3}$ a.u. at $R=5.18$ bohrs, in reasonable agreement with our result, $B_{21}=0.31 \times 10^{-3}$ a.u. However, empirical dipole strengths and ranges are not really suited to test the

theoretical results, and we thus proceed to the much more stringent tests based on spectral moments and spectral profiles for a more direct and more meaningful comparison of the new data with existing measurements.

SPECTRAL PROFILE

The theory of CIA line shapes has been reported previously.²⁴ It has been applied to the rototranslational spectra of H_2 -He (see Refs. 11 and 24) and many other systems.¹⁰ The extension of such work to rovibrational bands has not yet been attempted but is straightforward, with just three minor modifications. First, we replace the vibrational averages of the induced dipole moment $\langle v | A_{\lambda L} | v' \rangle$, with $v=v'=0$, by the appropriate vibrational matrix elements $v=0 \rightarrow v'=1$ as discussed above, Eq. (17) of Ref. 24. Second, for the rotational frequencies $\omega_{jj'}$ we substitute rovibrational frequencies

$$\omega_{vv'j'j} = (E_{v'j'} - E_{vj}) / \hbar \quad (5)$$

in Eq. (21) of Ref. 24. The rovibrational energy levels E_{vj} of the hydrogen molecule are well known.²⁵ Third, we account for the fact that the H_2 -He interaction potential depends on the vibrational coordinate r as described elsewhere.²⁶ Similarly as this was done for the computation of the $B_{\lambda L}$, Eq. (2), we expand the isotropic part $V_0(R, r)$ of Meyer, Hariharan, and Kutzelnigg's *ab initio* potential surface²⁶ for fixed R as a polynomial in $\rho=r-r_0$ and use the matrix elements $\langle v | r^n | v \rangle$, Table VII of Ref. 27, to compute the appropriate vibrational averages $\langle v | V_0(R, r) | v \rangle$ for $v=0$ and 1. In our line-shape computations, the tables of $\langle v | V_0 | v \rangle$ thus obtained were interpolated with the help of cubic spline polynomials. The extended Table I of Ref. 28 is used as input for a broad selection of tabulated $V_0(R, r)$ values. The vibrational averages of $V_0(R, r)$ for $v=0$ and 1 are significantly different and lead to different looking spectral profiles, in better agreement with the observation, than when the dependence of the interaction potential on the vibrational coordinates are ignored.

The H_2 -He *ab initio* interaction potential has been shown to be in excellent agreement with a number of discriminating measurements.^{26,28} We note that this potential does not support bound states or sharp scattering resonances at the energies of interest. This fact simplifies the line-shape calculations; only free states need to be considered. For the line-shape computations, we sum over 37 partial waves ($0 \leq l \leq 36$) at 300 K, and about twice as many at 3000 K. Over 15 000 radial matrix elements have been computed for the $\lambda L=01$ and 21 components, and

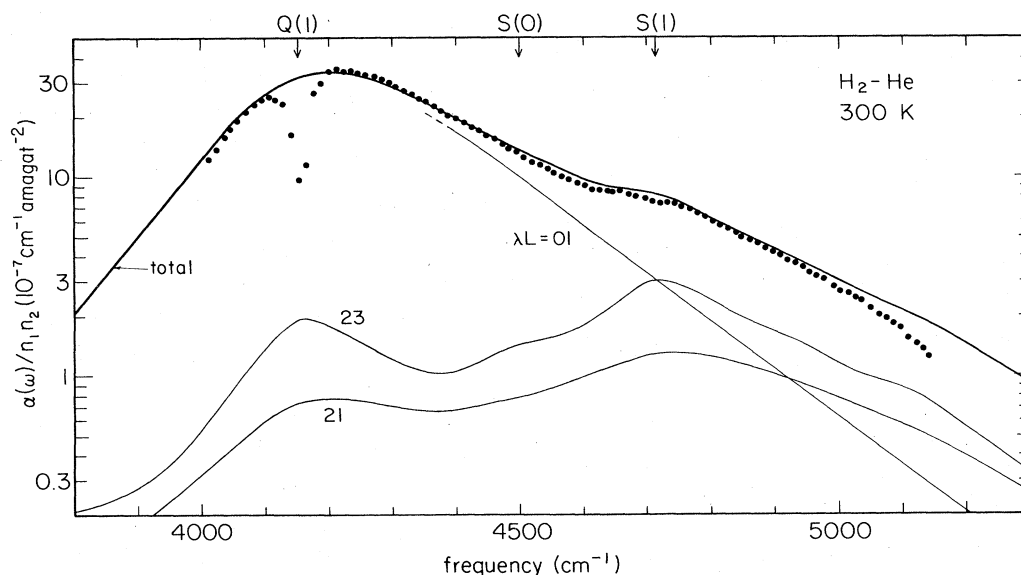


FIG. 2. Theoretical binary CIA spectrum of the rovibrational band at 300 K (heavy) and its three main components ($\lambda L=01$, 21, and 23); the $\lambda L=45$ component is less than $0.2 \times 10^{-7} \text{ cm}^{-1} \text{ amagat}^{-2}$ and therefore not shown. The dots represent Hunt's measurement (Ref. 29) (as shown in Ref. 30) at ~ 100 amagat total density and a $[\text{H}_2]:[\text{He}]$ abundance ratio of 1:20.

about 3 and 5 times as many for the $\lambda L=23$ and 45 components, respectively. The estimated numerical uncertainty of the line-shape calculation is in the 1% range.

Figure 2 compares the results of our computations at 300 K with Hunt's measurement²⁹ (as published in Ref. 30). The spectrum does not have many well-developed features. Only a broad, unresolved Q branch and a diffuse $S_1(1)$ line is seen, other lines [such as $S_1(j)$ with $j=0,2,3$] are barely discernible. Various dips of the measurement at 4126, 4154, and 4712 cm^{-1} are caused by intercollisional interference^{2,13-15} which as a many-body effect is absent in our binary theory. While the binary line shape is independent of density if normalized by the densities, $\alpha(\omega)/n_1 n_2$, the intercollisional dips are not, as explained elsewhere.²

In the framework of the isotropic potential approximation, the spectral contributions arising from the various $B_{\lambda L}$ induction operators shown in the figure are superimposed incoherently to form the curve marked "total." About 90% of the Q branch (in the broad vicinity of 4150 cm^{-1}) arises from the isotropic overlap induction ($\lambda L=01$). The anisotropic overlap component ($\lambda L=21$) is a little less than one-half as intense as the quadrupole induced term (23); these two components are responsible for the diffuse $S_1(1)$ -line structure superimposed on the broad isotropic induction component which is of roughly the same intensity near the $S_1(1)$ -line center.

We note that another recent measurement³¹ at 298 K does not agree with the theory as closely as Hunt's measurement shown in Fig. 2. While at low frequencies, from about 3900 to 4100 cm^{-1} , the agreement is excellent, we find an excess intensity at the higher frequencies: about 20% at 4300 cm^{-1} and increasing to 50% at 5000 cm^{-1} , for unknown reasons. Measurements at two other tem-

peratures of Reddy and Chang³¹ are in reasonable agreement with theory as we will see below when considering spectral moments.

Figures 3 and 4 compare the low-temperature measurements of McKellar *et al.*³² with theory. A mixture of parahydrogen and helium has been used so that our choice of an isotropic potential surface is fully justified; at these temperatures, only the $j=0$ state is populated. The very sharp observed $Q_1(0)$ intercollisional dips have been suppressed in the figures. Excellent agreement of measurement and theory is observed at these low temperatures except near the peak of the $S_1(0)$ lines where the measurement falls below theory by $\sim 10\%$, and an excess intensity is noticeable between 4650 and $\sim 4900 \text{ cm}^{-1}$. The observed excess is the $S_1(1)$ line of hydrogen arising from a residual $\sim 10\%$ ortho- H_2 concentration that could not be avoided in the measurement. This small ortho- H_2 concentration is also responsible for at least some part of the observed defect of the measured $S_1(0)$ -line peak intensity.

We note that the comparisons of theory and measurements are made on an absolute intensity scale; no scaling factors or other fitting parameters of any sort have been used. The observed consistency of the fundamental theory and the measurements shown is, therefore, quite remarkable. The agreement is typically better than 10%, our estimate of the experimental uncertainties, except near the intercollisional dips caused by many-body interactions which are not accounted for in the binary theory. This agreement is comparable to similarly close agreements observed previously between measurements and the fundamental theory in the rototranslational bands.¹¹ These results demonstrate that the quantum chemical SCF and CEPA methods are capable of providing very accurate data for the induced dipoles, with uncertainties of the best

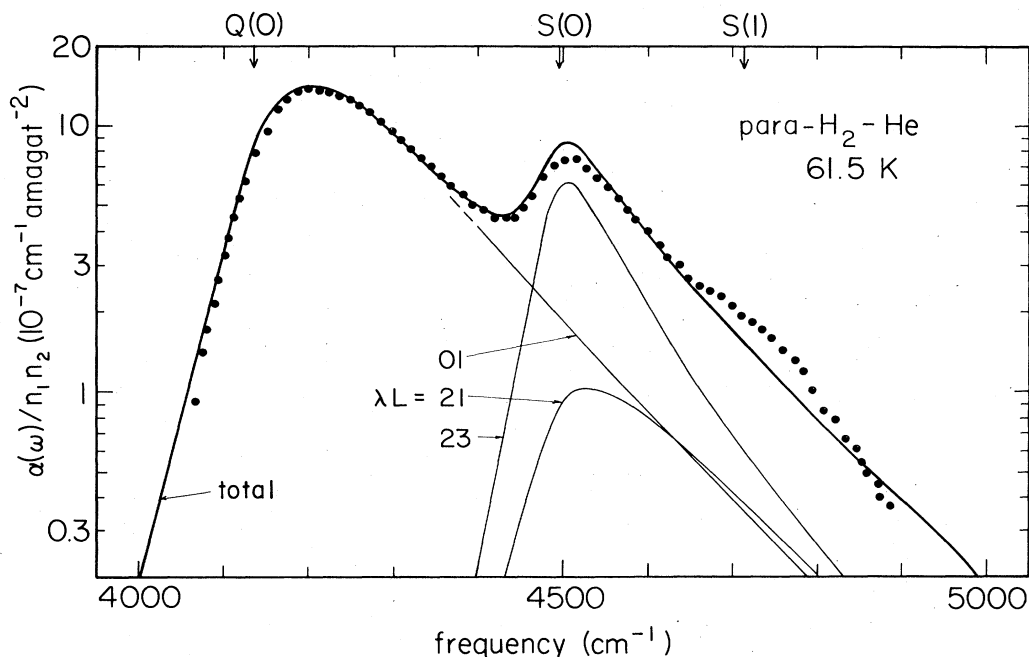


FIG. 3. Theoretical binary CIA spectrum of the rovibrational band at 61.5 K (heavy) and its three main components ($\lambda L=01$, 21, and 23); the $\lambda L=45$ component is less than $0.2 \times 10^{-7} \text{ cm}^{-1} \text{ amagat}^{-2}$ and therefore not shown. The dots represent the measurement of McKellar *et al.* (Ref. 32) at a para- H_2 and helium density of 1.1 and 52 amagat, respectively.

computations in the 2% range.

In the absence of measurements of CIA spectra of H_2 -He at high temperatures, Linsky⁶ has attempted a prediction of the spectra by some empirical extrapolation procedure. For comparison, we show our results at temperatures from 600 to 30000 K in Fig. 5. Near peak absorption, at 600 and 3000 K, our results are 50% and 400% more intense than the estimate⁶ suggests; furthermore, the shapes of the profiles and their temperature dependence

are quite different. The data presented here allow a much more accurate, dependable prediction of the absorption spectra than hitherto possible.

SPECTRAL MOMENTS

Moments of the rovibrational spectra are defined by

$$\alpha_1 = \frac{1}{n_1 n_2} \int \alpha(\omega) d\omega, \quad (6)$$

$$\gamma_1 = \frac{\hbar}{2kTn_1 n_2} \int \alpha(\omega) \frac{d\omega}{\omega}. \quad (7)$$

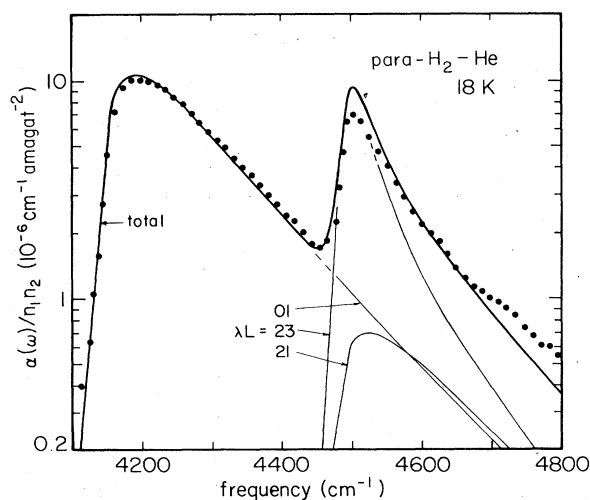


FIG. 4. Theoretical binary CIA spectrum of the rovibrational band at 18 K (heavy) and its three main components ($\lambda L=01$, 21, and 23); the $\lambda L=45$ component is less than $0.2 \times 10^{-7} \text{ cm}^{-1} \text{ amagat}^{-2}$ and therefore not shown. The dots represent the measurement of McKellar *et al.* (Ref. 32) at 1.1 and 52 amagat, respectively.

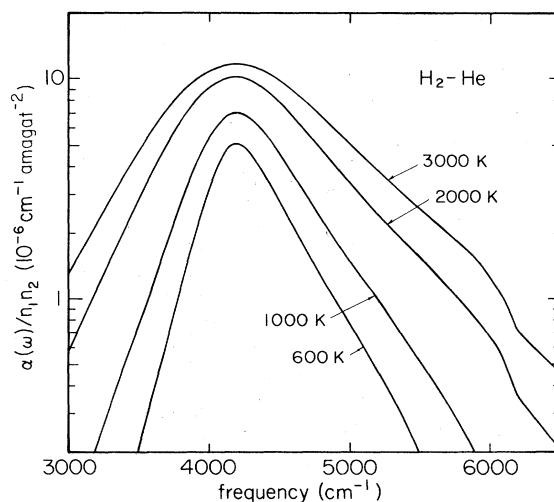


FIG. 5. Theoretical binary CIA spectra of the fundamental band at temperatures from 600 to 3000 K.

In these expressions, $\alpha(\omega)$ is the absorption coefficient in units of cm^{-1} , n_1 and n_2 are the number densities of H₂ and He, respectively, $\omega = 2\pi c\tilde{\nu}$ is the frequency in radians per second, $\hbar = 1.05 \times 10^{-34}$ J sec is Planck's constant, and kT designates the thermal energy as usual. The integrals are to be taken over the complete fundamental band.

These moments are computable from molecular parameters, the induction components $B_{\lambda L}$ and the interaction potential,²² but in our case it was convenient to obtain these by integration of the computed spectra $\alpha(\omega)$. In previous work,⁹⁻¹¹ we have compared the spectral integrals [like Eqs. (6) and (7)] with exact sum formulas obtained from a numerical quantum computation of high precision.³³ Very close agreement, at the level of 1%, was achieved in every case in such computations for the lowest three moments. The precision of the present line-shape computation is believed to be the same as in previous work. We note that the computed values of α_1 and γ_1 do not depend on whether mixtures of equilibrium hydrogen, normal hydrogen or parahydrogen with helium are considered. The results are shown in Figs. 6 and 7. Spectroscopists usually determine α_1 or γ_1 , sometimes both, from their measurements. We have, therefore, plotted the available experimental moments for a more comprehensive comparison with theory. We note that in many publications, spectral profiles are often reproduced quite small so that an accurate reading of measured spectra is difficult if not impossible. The spectral moments α_1 and γ_1 , on the other hand, do not suffer from the shortcomings of published figures and reflect better the precision of the measurement. The low-temperature measurements by McKellar *et al.*,³² and by Watanabe and Welsh,³⁰ are seen to be in close agreement with the theory. The measurements by Reddy and Chang³¹ at 77 and 273 K are also in excellent agreement, but at 195 and 298 K, the inferred moments are 20% to 25% greater than the fundamental theory, for an unknown reason; the measured profiles at 195 and 298 K are also inconsistent with the computed line shapes as was mentioned above.

For the spectral moments, virial expansions of the form

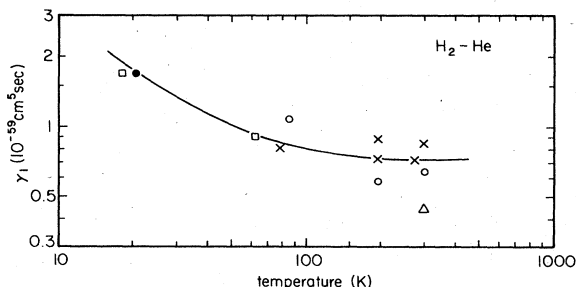


FIG. 6. Spectral moment γ_1 of the H₂-He fundamental band as function of temperature. The curve represents the theoretical results. Measurements: dots, Watanabe and Welsh (Ref. 30); open circles, Hunt (Ref. 29); \times , Reddy and Chang (Ref. 31); squares, McKellar *et al.* (Ref. 32); triangles, Hare and Welsh (Ref. 35).

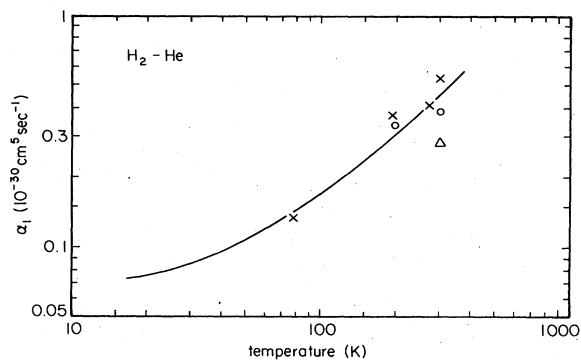


FIG. 7. Spectral moment α_1 of the H₂-He fundamental band as function of temperature. The curve represents theory. Measurements: open circles, Chisholm and Welsh (Ref. 34); \times , Reddy and Chang (Ref. 31); triangles, Hare and Welsh (Ref. 35).

$$\alpha_1 = \alpha_1^{(2)} n_1 n_2 + \alpha_1^{(3)} n_1 n_2^2 + \dots \quad (8)$$

exist, similarly for γ_1 . Where these were specified, we have plotted the binary coefficients $\alpha_1^{(2)}$ and $\gamma_1^{(2)}$; see, for example, Chisholm and Welsh.³⁴ Our theory provides of course just the binary moments $\alpha_1^{(2)}$ and $\gamma_1^{(2)}$. If the measurements were taken at low densities, a virial expansion is not necessary and the experimental values are used without corrections. The work by Hare and Welsh³⁵ was done at the highest densities (1500 to 5000 atm at 300 K). It involves substantial extrapolation to the low-density limit, rendering the resultant binary moments perhaps less dependable than other work (triangles, Figs. 6 and 7). Apart from such extreme cases, the apparent scatter of the measured moments illustrates the magnitude of the experimental uncertainties. The theoretical curves are near the average of these measurements and, in that sense, are nicely supported by the measurements.

We note that the previous *ab initio* work²¹ provides a value of the moment γ_1 at 61.5 K which is $\sim 40\%$ greater than our results. Linsky⁶ estimates $\gamma_1 = 8 \times 10^{-60}$ cm^5/sec at 600 K, and a $T^{-0.451}$ or $T^{-0.5}$ temperature dependence at the higher temperatures. We find $\gamma_1 = 7.7, 8.3, 9.5,$ and 11×10^{-60} cm^5/sec at 600, 1000, 2000, and 3000 K which suggests a different temperature dependence, namely, an increase with temperature rather than a decrease. A glance at Fig. 6 shows that γ_1 decreases with temperature at low temperatures. It goes through a broad minimum near $T \approx 500$ K and increases with temperature above that.

CONCLUSION

Spectral profiles of rotovibrational spectra have been obtained from the fundamental theory for the first time in this work. We have seen that existing measurements of the collision-induced fundamental band of H₂-He generally agree within the experimental uncertainties with the re-

sults of the fundamental theory over the range of temperatures from 18 to 300 K. Theory can thus be used with confidence to dependably predict such spectra at temperatures where no measurements exist, and perhaps predict similar collision-induced overtone and hot bands of the H₂-He complex which apparently have never been measured in the laboratory. This is an important point

for many astrophysical applications where such spectra must be modeled accurately as functions of temperature.

ACKNOWLEDGMENT

One of us (L.F.) acknowledges support from the National Science Foundation under Grant No. AST 8310786.

- ¹M. F. Crawford, H. L. Welsh, and J. L. Locke, *Phys. Rev.* **75**, 1067 (1949).
- ²H. L. Welsh, in *MTP International Review of Science, Physical Chemistry, Series I*, edited by A. D. Buckingham and D. A. Ramsay (Butterworths, London, 1972), Vol. 3, p. 33.
- ³J. D. Poll, *Intermolecular Spectroscopy and Dynamical Properties of Dense Systems*, edited by J. van Kranendonk (Società Italiana di Fisica, Bologna, Italy, 1980), pp. 45–76.
- ⁴L. Trafton, *Astrophys. J.* **179**, 971 (1973).
- ⁵R. H. Tipping, *Phenomena Induced by Intermolecular Interactions*, edited by G. Birnbaum (Plenum, New York, 1985), p. 727.
- ⁶J. L. Linsky, *Astrophys. J.* **156**, 989 (1969).
- ⁷H. L. Welsh, *J. Atmos. Sci.* **26**, 835 (1969).
- ⁸W. Meyer, *Phenomena Induced by Intermolecular Interactions*, edited by G. Birnbaum (Plenum, New York, 1985), p. 29.
- ⁹W. Meyer and L. Frommhold, *Phys. Rev. A* **33**, 3807 (1986).
- ¹⁰J. Borysow and L. Frommhold, *Phenomena Induced by Intermolecular Interactions*, edited by G. Birnbaum (Plenum, New York, 1985), p. 67.
- ¹¹W. Meyer and L. Frommhold, *Phys. Rev. A* **34**, 2771 (1986).
- ¹²S. P. Reddy, *Phenomena Induced by Intermolecular Interactions*, edited by G. Birnbaum (Plenum, New York, 1985), p. 129.
- ¹³J. van Kranendonk, *Can. J. Phys.* **46**, 1173 (1968).
- ¹⁴J. van Kranendonk, *Intermolecular Spectroscopy and Dynamical Properties of Dense Systems*, edited by J. van Kranendonk (Società Italiana di Fisica, Bologna, Italy, 1980), p. 77.
- ¹⁵J. C. Lewis, *Phenomena Induced by Intermolecular Interactions*, edited by G. Birnbaum (Plenum, New York, 1985), p. 215.
- ¹⁶J. L. Hunt and H. L. Welsh, *Can. J. Phys.* **42**, 873 (1964).
- ¹⁷J. W. MacTaggart and H. L. Welsh, *Can. J. Phys.* **51**, 158 (1973).
- ¹⁸W. Kolos and L. Wolniewicz, *Can. J. Phys.* **53**, 2189 (1975).
- ¹⁹A. Dalgarno and A. E. Kingston, *Proc. R. Soc. London, Ser. A* **259**, 424 (1960).
- ²⁰J. L. Hunt, J. D. Poll, and L. Wolniewicz, *Can. J. Phys.* **62**, 1719 (1984).
- ²¹P. E. S. Wormer and G. van Dijk, *J. Chem. Phys.* **70**, 5695 (1979).
- ²²J. D. Poll and J. L. Hunt, *Can. J. Phys.* **54**, 461 (1976).
- ²³J. D. Poll, J. L. Hunt, and J. W. MacTaggart, *Can. J. Phys.* **53**, 954 (1975).
- ²⁴G. Birnbaum, S. I. Chu, A. Dalgarno, L. Frommhold, and E. L. Wright, *Phys. Rev. A* **29**, 595 (1984).
- ²⁵G. Herzberg, *Spectra of Diatomic Molecules* (Van Nostrand, Princeton, 1962).
- ²⁶W. Meyer, P. C. Hariharan, and W. Kutzelnigg, *J. Chem. Phys.* **73**, 1880 (1980).
- ²⁷L. Wolniewicz, *J. Chem. Phys.* **45**, 515 (1966).
- ²⁸J. Schaefer and W. E. Köhler, *Physica* **129A**, 469 (1985).
- ²⁹J. L. Hunt, Ph.D. thesis, University of Toronto, 1959 (unpublished).
- ³⁰A. Watanabe and H. L. Welsh, *Can. J. Phys.* **43**, 818 (1965).
- ³¹S. P. Reddy and K. S. Chang, *J. Mol. Spectrosc.* **47**, 22 (1973).
- ³²A. R. W. McKellar, J. W. MacTaggart, and H. L. Welsh, *Can. J. Phys.* **53**, 2060 (1975).
- ³³M. Moraldi, A. Borysow, and L. Frommhold, *Chem. Phys.* **86**, 339 (1984).
- ³⁴D. A. Chisholm and H. L. Welsh, *Can. J. Phys.* **32**, 291 (1954).
- ³⁵W. F. J. Hare and H. L. Welsh, *Can. J. Phys.* **36**, 88 (1958).